creative commons
COMMONS DEED

저작자표시 2.0 대한민국

이용자는 아래의 조건을 따르는 경우에 한하여 자유롭게

- 이 저작물을 복제, 배포, 전송, 전시, 공연 및 방송할 수 있습니다.
- 이차적 저작물을 작성할 수 있습니다.
- 이 저작물을 영리 목적으로 이용할 수 있습니다.

다음과 같은 조건을 따라야 합니다:

저작자표시. 귀하는 원저작자를 표시하여야 합니다.

- 귀하는, 이 저작물의 재이용이나 배포의 경우, 이 저작물에 적용된 이용허락조건을 명확하게 나타내어야 합니다.
- 저작권자로부터 별도의 허가를 받으면 이러한 조건들은 적용되지 않습니다.

저작권법에 따른 이용자의 권리는 위의 내용에 의하여 영향을 받지 않습니다.

이것은 이용허락규약(Legal Code)을 이해하기 쉽게 요약한 것입니다.

Disclaimer

dCollection

Master's Thesis of Engineering

Deposition of Liquid Metal Thin Film Patterns for Stretchable Electronics Using Thermal Evaporation

신축성 전자 장치 개발을 위한 열 증발 방식을 이용한 액체 금속 박막 패턴 증착

February 2019

Graduate School of Engineering
Seoul National University
Mechanical Engineering Major

YeongHyeon Jeong

Deposition of Liquid Metal Thin Film Patterns for Stretchable Electronics Using Thermal Evaporation

Advisor Yong-Lae Park

Submitting a master's thesis of Public Administration

October 2018

Graduate School of Engineering
Seoul National University
Mechanical Engineering Major

YeongHyeon Jeong

Confirming the master's thesis written by
YeongHyeon Jeong
December 2018

Chair	Jong-Won Kim	(Seal)
Vice Chair	Yong-Lae Park	(Seal)
Examiner	Suk-Won Cha	(Seal)

Abstract

Advances in soft robotics have led to greater demand for highly deformable and lightweight sensors in various applications with the characteristics of high flexibility and stretchability, durability, and biocompatibility. Most processes in the fabrication of soft electronics are manual and thus time-consuming. In this paper, to satisfy the requirements of soft sensors and to improve the conventional manual process of soft electronics fabrication, a novel fabrication method for the creation of soft sensors using thermal evaporation is proposed. The proposed fabrication process involves the handling of two thin solid-phase films compared to the conventional method of controlling liquid-phase metal, thus leading to better step coverage, lower costs and reduced processing time. Moreover, a manual process is not required, implying that automation processes and mass production are feasible. The conventional method takes about 8~9 hours, whereas the proposed method reduces the time by half (about 4~5 hours). Handling solid phase elements prevents the leakage of the liquid metal during the manufacturing process. This paper mainly addresses the soft sensor fabrication process using thermal evaporation in comparison with the conventional fabrication method. Chapter 1 presents the

background of the study and the overall process summary. Chapter 2 describes the steps of the overall fabrication process and explains the problems with the process and the related solutions. Chapter 3 shows the results of testing of the thermally evaporated sensor and its characterization. Chapter 4 discusses a comparison of the conventional injection method and the proposed method. Finally, chapter 5 concludes the paper by covering the strengths and weaknesses of the proposed method while also discussing future work.

Keyword: Soft sensor, Fabrication, Thermal evaporation, Deposition, Automation, Mass production

Student Number: 2017-29518

Table of Contents

Chapter 1. Introduction 1

Chapter 2. Process Design 5

2.1. Characteristics of Gallium and Indium

2.2. Shadow Mask

2.3. Deposition onto PDMS

2.4. Deposition Thickness

2.5. Thermal Evaporation Condition

2.6. Whole Fabrication Process

Chapter 3. Result 19

3.1. Sensor Characterization

Chapter 4. Discussion

Chapter 5. Conclusion

Bibliography 26

Abstract (Korean) 34

Chapter 1. Introduction

The appearance of soft robots and wearable devices has caused people to become interested in skin-mountable and stretchable electronics. Among these electronics, soft sensors are well known for its high flexibility, durability, biocompatibility, and lightweight characteristics [1] [2].

Soft sensors are fabricated in many different ways. Most fabrication methods use liquid metal to maintain conductivity during deformation, including filtration [3] [4], printing [5] [6], coating [7] [8], liquid-phase mixing [9] [10], chemical synthesis [11] [12], and transferring and micro-molding [13] [14] [15]. Among these methods, injecting the liquid metal after the creation of the mold is one of the most common ways to fabricate a soft sensor due to its simplicity [16]. From a 3D-printed mold, an elastomer is poured and cured. The cured elastomer is then laminated with another layer, and then eutectic gallium-indium (EGaIn), a conductive material, is injected between the top and bottom elastomer layers under pressure [28].

EGaIn, a conductive liquid material, is popular for use in soft wearable robot applications [17]. This conductive material is easily found in flexible sensors or stretchable electronics. EGaIn is an

alloy of gallium (Ga) and indium (In) which maintains in a liquid state at room temperature. EGaIn is also ideal for soft sensor fabrication due to its high surface tension and electric conductivity [18]. However, the soft sensor fabrication method using EGaIn injection has several disadvantages. The first involves limitation in mass production and automation, as all the processes require human labor. In addition, due to the manual process, the production rate is very low and time-consuming. Another problem is uniformity. Manual injection of liquid metal does not guarantee the same amount of liquid metal filled in the sensor, thus lowering the repeatability of multiple sensor. Moreover, management and control of the liquid metal are challenging, especially considering that the liquid metal may contaminate both the work space and the processor.

To solve these problems, EGaIn, which consists of gallium and indium, as mentioned above, was deposited by thermal evaporation while remaining as a thin solid-phase film. Owing to the low melting temperature of gallium, the thermal evaporator power source had to be modulated to operate in a low temperature range. Substrates were patterned through the shadow mask method. The shadow mask was ideal for applications at lower resolutions, where alignment to previous layers was not critical, and the elimination of multiple processing steps added value by reducing the cost and

reducing the processing time. For a spindly and meandering microchannel shape, adhesive Kapton tape replaced the typical metal shadow mask. The Kapton mask was patterned with a laser cutter, and the critical parameters of the laser cutter were set such that the laser did not scratch the substrate. The parameters were selected after several trial-and-error cycles. Additionally, deposited metal onto PDMS was generally poor. A surface treatment while engraving and adding a bonding layer with titanium were key aspects of the deposition process. After depositing the thin gallium and indium layers, the Kapton mask was eliminated. At this point, applying pressure caused the two solid films to become one liquid phase, which also provided sensitive conductivity. Moreover, the thickness of the deposited film of gallium was 150nm and that of indium is 40nm. These thin films were able to be utilized as thin, sensitive and stretchable soft sensors.

There is still room for improvement. Various patterning methods should be tested, and refinement of the fabrication process is necessary to improve the sensor uniformity and performance. Moreover, different types of shadow mask should be found because the Kapton mask is disposable.

The major contribution of this research is to propose a fabrication method that can control the solid-phase materials

before their liquidation. This leads to improvements in the overall fabrication process, time required, and cleanliness of the working space. The other contribution is that this novel fabrication method does not require human labor and can thus allow automation processes and mass production while also saving significant amounts of time.

Chapter 2. Process Design

2.1. Characteristics of Gallium and Indium

The melting points of Ga and In are 29.76℃ and 156.6℃, respectively. EGaIn, an alloy of Ga and In, is known to melt at around 15℃, as summarized in Table 1. Due to this characteristic, it remains in a liquid phase at room temperature. Given that controlling a solid-phase material is much easier than controlling a liquid phase material, the solid phase of Ga and In is deposited using a thermal evaporator. These two thin layers become a liquid metal by applying a mechanical stimulus, such as pressure. Handling the liquid metal causes leakage and contamination of the work space and poses a hazard to people in the laboratory. However, using thermally two evaporated layers can prevent this problem.

TABLE 1

Material Properties

	Gallium	**Indium**	**EGaIn**
Melting Point	29.76°C	156.6°C	15°C

2.2. Shadow Mask

Although there are several methods for micro-patterning, the shadow mask was chosen for its simple fabrication process [19]. A shadow mask is a thin sheet of metal with a pattern, placed into close contact with the substrate. The thin film material is deposited directly onto the substrate through the mask. This technique is ideal for applications with relatively low resolutions, where alignment to previous layers is not critical, and the elimination of multiple processing steps adds value by reducing the cost and reducing the processing time [29]. The thin sheet of the metal mask introduces a problem when it is designed for a thin and long meandering microchannel because it hangs down as a hair would, which thus causes it to lose its role as a shadow mask [30]. To address this issue, adhesive Kapton tape was selected as a substitute [20]. Kapton is a type of polyimide film that remains stable across a wide range of temperatures from −269 to +400℃. Hence, Kapton tape is structurally safe inside a thermal evaporator.

The other issue to consider when using Kapton tape as a shadow mask is the laser cutting parameters (Speedy 300 fle, Trotec). During the patterning step, the shadow mask of the Kapton tape adheres to the substrate. Because the two layers are in contact, proper adjustment of the laser cutter parameters is necessary to

cut not the substrate but only the mask [31]. If the speed is increased, the time per unit length will be decreased and the influence of heat around the desired patterning will be reduced. If the speed is lowered, although the accuracy is increased, the increased time will cause unwanted heat transfer to other patterning areas. Therefore, proper adjustment of the parameters is very important during the patterning step. Figure 1 shows the trial-and-error process used to select the parameters of the laser cutter. From Figure 1-e, parameters which leave cutting traces are not suitable these settings cause scratches on the substrate. Figure 1-d indicates that as the speed increases, the exposure time of the laser cutter per unit length is reduced. Therefore, cutting is not performed properly. After the trial-and-error process, the best settings for the laser cutter parameters were as follows: power of 25 and a speed of 5, or power of 40 and a speed of 10.

(a) Adjustment of power & speed parameters

Speed \ Power	5	10	15	20	25	30	35	40
1								
5								
10								
15								
20								

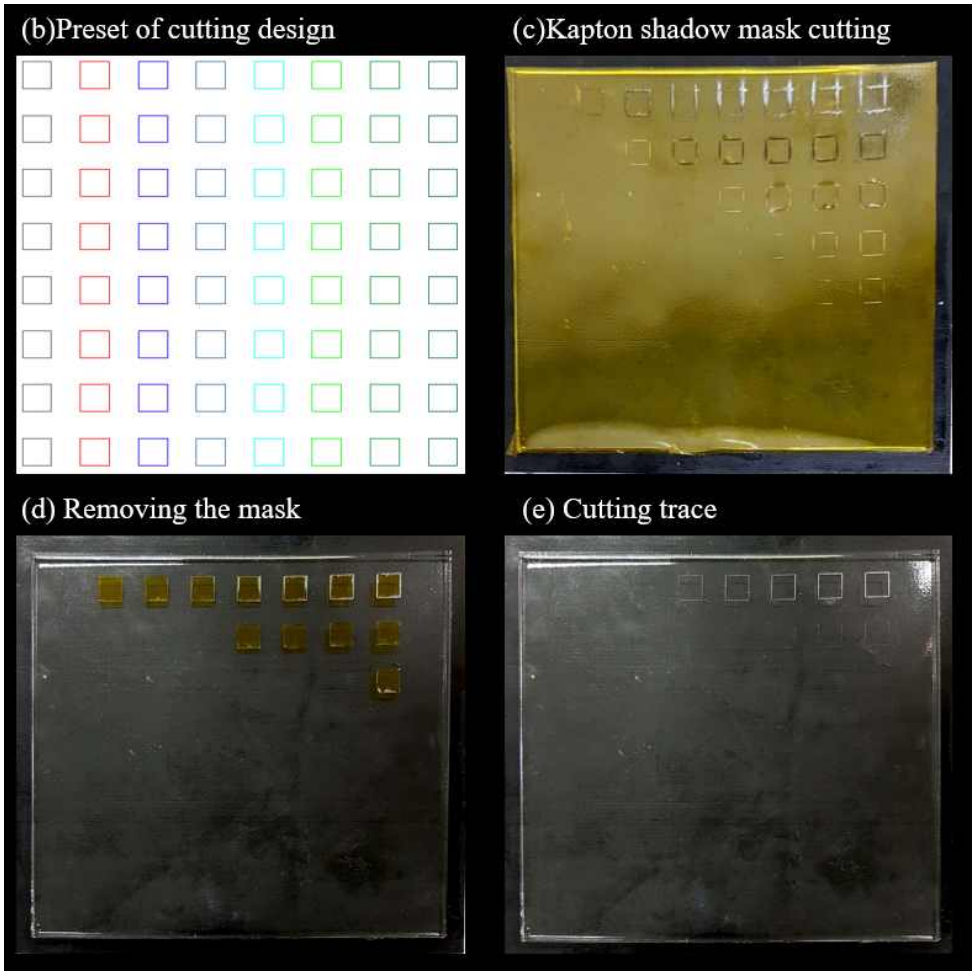

Fig. 1. The laser cutter parameter selection, (a) adjustment variable power and speed, (b) preset of cutting design, (c) actual cutting of the kapton mask with the laser cutter, (d) the result of removing the shadow mask, (e) the cutting trace after getting rid of all the kapton.

2.3. Deposition onto PDMS

PDMS is known for poor metal adhesion [21], creating metal aggregates due to its high surface hydrophobicity [22]. The hydrophobicity of PDMS causes dissociated islands of a thin metal film or cracks, making it difficult to evaporate metal onto PDMS. The other characteristic of PDMS is its ability to absorb hydrophobic small molecules [23]. When metals are evaporated onto PDMS, its unique features give rise to discontinuities in the evaporated thin metal film. In order to address these issues, titanium is used as a sacrificial and bonding layer [24]. Generally, titanium helps with adhesion between a metal layer and an elastomer, in addition to imparting the benefits of improving the wear and degree of biocompatibility [25].

Another way to enhance adhesion onto PDMS is to increase the roughness of the surface [26]. The smoother the surface of PDMS is, the higher the hydrophobicity of the surface becomes. In order to demonstrate this phenomenon, an engraved mold was prepared to make a rough surface PDMS. Figure 2 presents the engraved acrylic mold and cured PDMS on the mold. Figure 3 shows the clear difference in the deposition of gallium and indium layers due to the presence or absence of the titanium layer and surface

roughness. Figure 3 indicates that the deposition of a Ti layer and increased roughness of the surface by engraving the mold helps gallium and indium to be deposited onto the PDMS. Figures 3-(c) and (d) indicate that without a titanium layer, gallium and indium cannot readily be deposited onto PDMS.

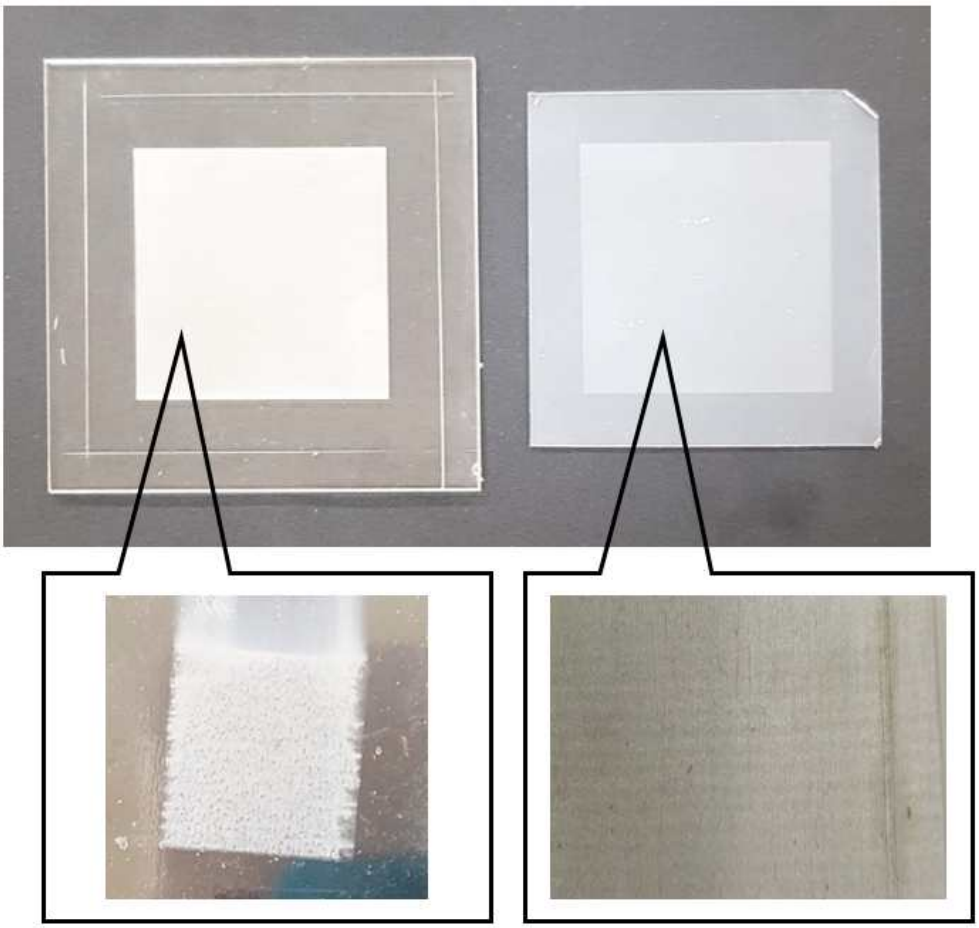

Fig. 2. Engraved acryl mold and cured PDMS on the mold

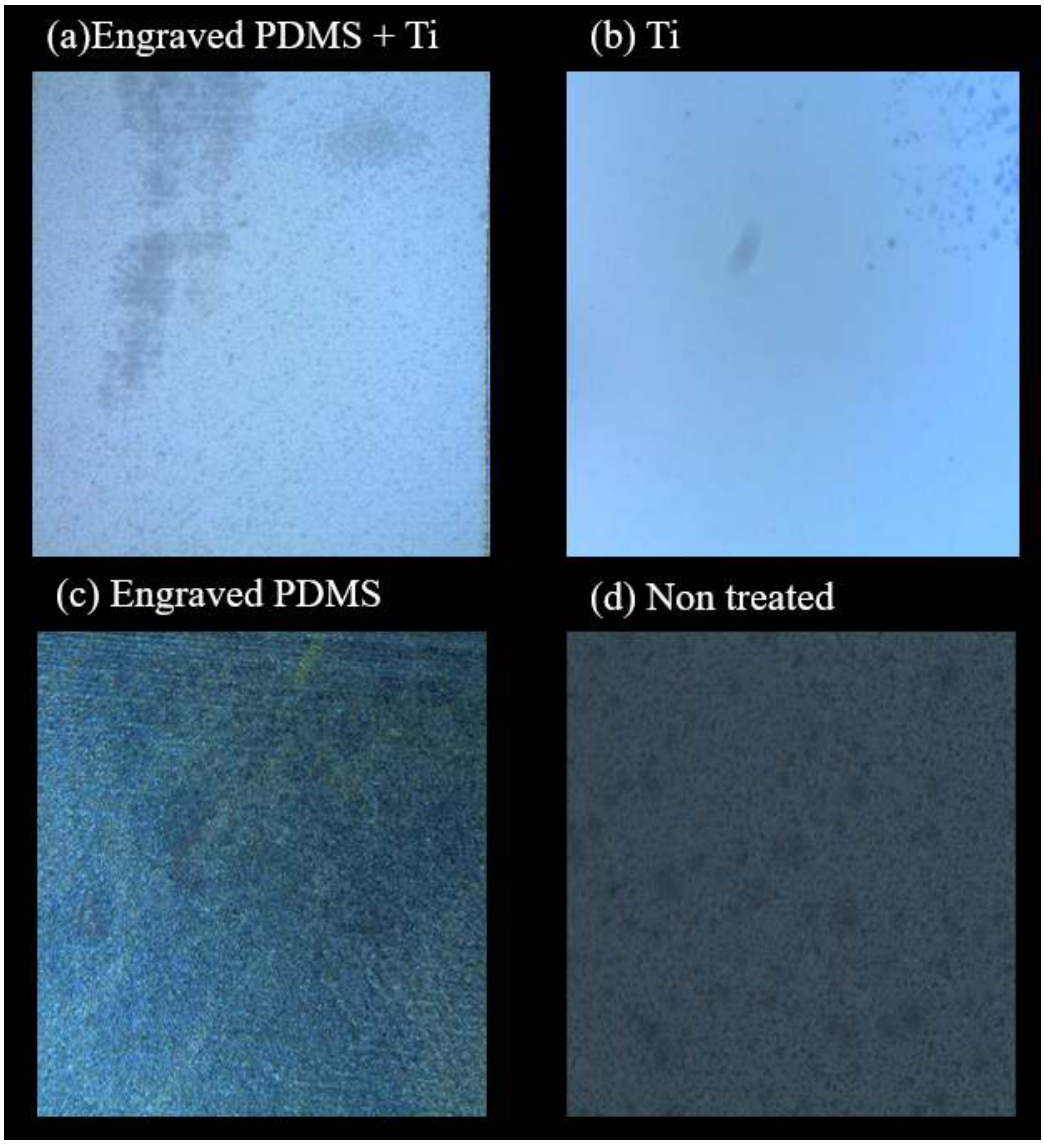

Fig. 3. Deposition of Ga and In, (a) engraved PDMS and deposited titanium layer, (b) deposited titanium as the sacrificial layer, (c) only engraved PDMS before Ga and In deposition, (e) normal PDMS.

2.4. Deposition Thickness

Gallium–indium eutectic (EGaIn) is an electrically conductive fluid metal [32]. It consists of 75.5% Ga and 24.5% In by weight. The densities of Ga and In are 5.91 g/cm³ and 7.31 g/cm^3, respectively. The thickness ratio calculated according to the density and weight ratio is 3.75: 1. To check the minimum thickness of the thin layer for the two thin solid–phase layers to become one liquid–phase layer, gallium and indium were deposited at a ratio of 3.75:1 stepwise from 10 nm of indium to 100 nm of indium. It was found that the optimum thickness was 40 nm of indium and 150 nm of gallium after an exhaustive search.

2.5. Thermal Evaporation Condition

A vacuum thermal evaporator was utilized to deposit titanium, gallium and indium at about 5 X 10–7 torr. The melting point of titanium was 1,668℃, whereas those of gallium and indium were very low. In order to control the two temperatures given the large gap, two different power sources were required for fine tuning. For a high melting temperature, a 380 V – 50 A power source was used and for a relatively low melting temperature, a 220 V – 50 A

power source was operated [33]. The deposition rate of each material was limited to 1 Å/s.

2.6. Overall Fabrication Process

A 10:1 ratio of PDMS was poured into the engraved acryl mold. It was cured for about 3~4 hours in a 60℃ oven. After the curing process, Kapton tape as the shadow mask was attached onto the PDMS. Patterning on the mask was performed using a laser cutter, after which the soot from the cutting process was removed with alcohol. The clearly patterned substrate was then put into the evaporator. The deposition started in a vacuum chamber below 5 X 10−7 torr. First, using a high−power source due to its high melting temperature, titanium was deposited to a thickness of 30 nm as a sacrificial layer and a bonding layer at the same time. After the titanium layer deposition process was finished, the subsequent deposition steps began in the order of gallium, indium, and gallium again at 75 nm, 40 nm, and 75 nm, respectively. Gallium was deposited twice to increase the contact area between gallium and indium. The increased contact area accelerated the transformation of the solid phase into the liquid phase and helps to form a more uniform surface. After all deposition steps were completed, the disposable shadow mask was eliminated and a signal wire was connected to the deposited area. Finally, the substrate was sealed

with another PDMS layer. Figure 4 depicts the automated, mass-producible overall fabrication process of the soft sensor using thermal evaporation. Figure 5-(a) shows the PDMS substrate with the Kapton shadow mask patterned with the laser cutter, and Figure 5-(b) is the final result after all the processes were finished.

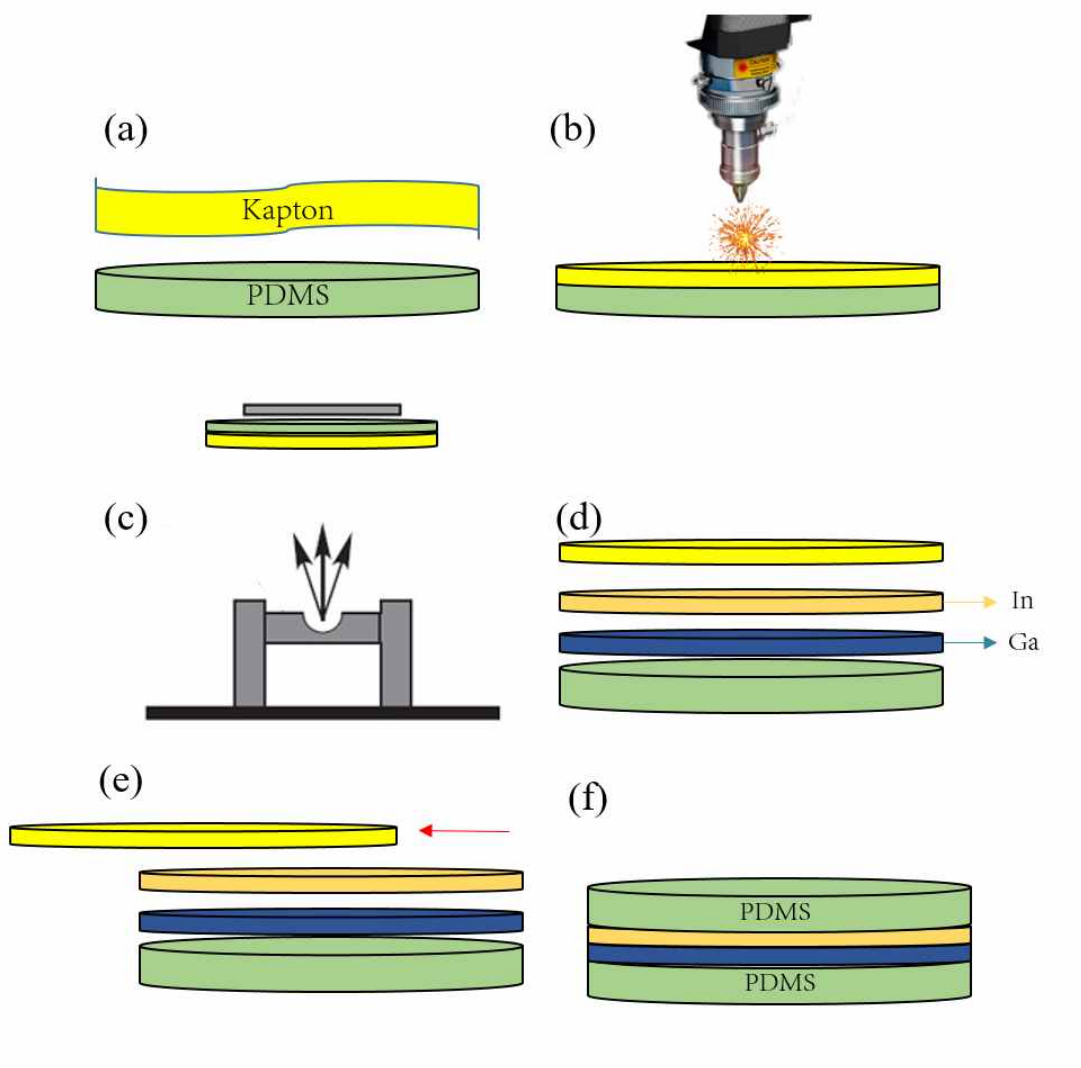

Fig. 4. The entire soft sensor fabrication process, (a) attachment of kapton tape to the PDMS, (b) patterning with the laser cutter, (c) evaportation of Ga and In, (d) apperance after the depostion process, (e) removing the mask, (f) sealing with the other PDMS layer.

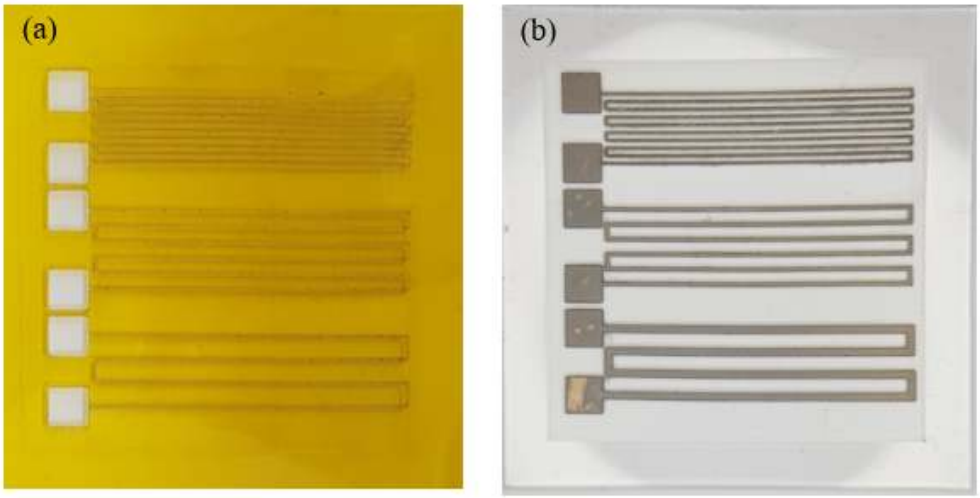

Fig. 5. (a) Kapton shadow maks patterned with laser cutter, (b) Soft sensor fabricated by thermal evaporation.

Chapter 3. Results

3.1. Sensor Characterization

To meet the necessary characteristics of a soft sensor, the sensor should be durable and flexible. To confirm the performance of the prototyped sensor, ten repeated tensile tests were conducted for a single representative sensor. For the test equipment, a motorized materials tester (ESM303, Mark-10) (Figure 6), was used, and the sensor dimensions were 50 mm wide, 50 mm long and 5 mm thick. Since PDMS is able to display elastic behavior up to a strain level of 40% [27], a strain level of 20% was chosen out of safety concerns. The spring constant of the sensor was 549 N/m, because when designing a sensor to prevent destruction, the thickness was set sufficiently high, leading to an increase in the stiffness of the sensor. Figure 7 displays the mechanical behavior of the sensor. One of the important aspects was the lack of change in the sensor characteristics during the trials.

Figure 8 shows the electrical response to strain of the fabricated sensor. This outcome indicates very low hysteresis and sensitivity. Although the sensor did not show a significant performance enhancement compared to conventional sensors, it demonstrated the promise that this fabrication method had room for improvement.

The linear fit estimates the sensor behavior very well (R^2 = 0.9867). Although there was still room for improvement of the sensor behavior, the mechanical and electrical responses both showed that the proposed sensor fabrication method using thermal evaporation was able to replace the conventional fabrication method of soft sensors with better results.

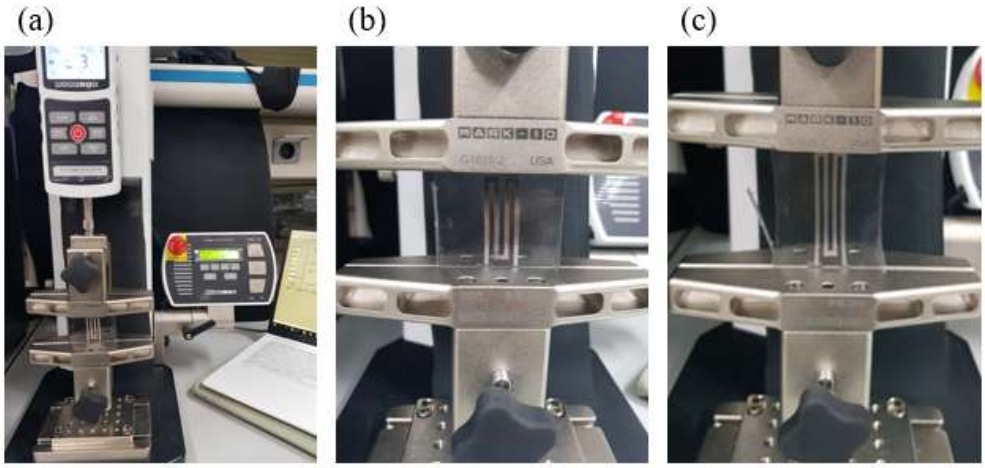

Fig. 6. Mechanical response to strain, (a) force measurement stand(Mark-10, ESM303), (b) initial status, (c) 20% strain.

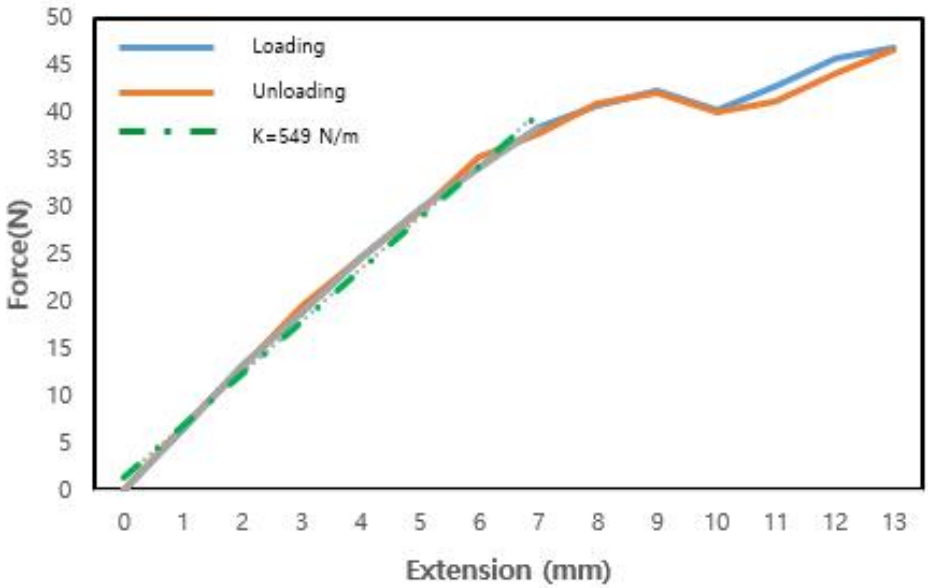

Fig. 7. The results of extension test for a single representative sensor. The extension rates in both loading and unloading cases are 1.25mm/s. the dashed lines are fitted to the linear areas to figure out the stiffness of the sensor.

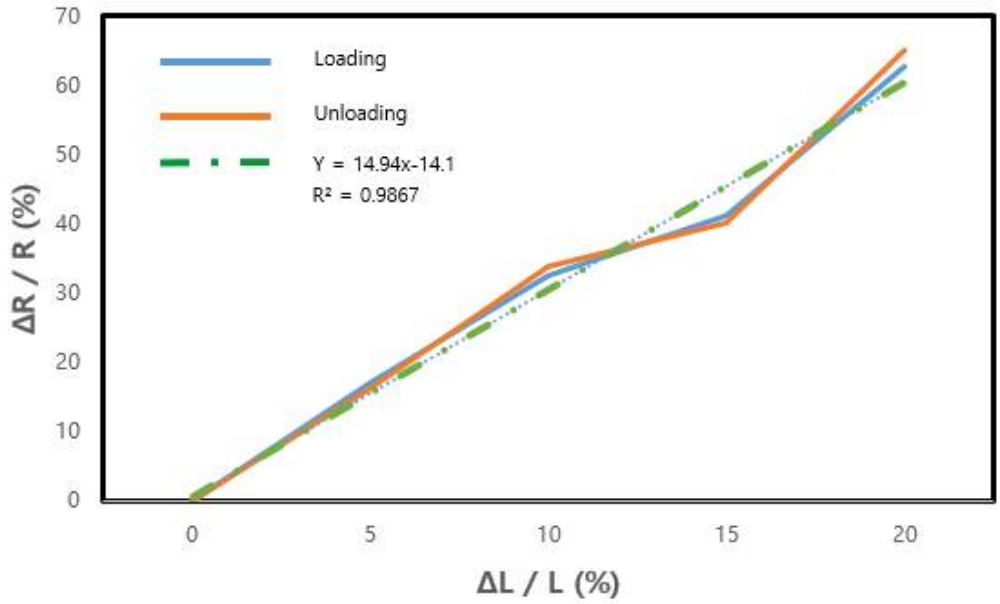

Fig. 8. The normalized sensor signal with high repeatability and low hysteresis. A linear fit to the proportional region of the signal shows a gain (slope) of 14.94%.

Chapter 4. Discussion

As mentioned earlier, the purpose of this study is to enhance the fabrication process of soft sensors made of elastomer and embedded liquid-metal microchannels so that automation and mass-production are possible. Table 2 shows the results of a comparison of the manufacturing times between the conventional injection-type fabrication method and the thermal evaporation method. The most time-consuming process in the conventional method was patterning with a 3-D printed mold. Once the mold was printed, even if it was reusable, it was possible to fabricate only sensors with the same shape. Therefore, small changes or adjustments are impossible. In addition, the time required for printing is 3~4 hours to create a 5x5 cm mold [35]. On the other hand, the patterning process of the novel fabrication method introduced here with thermal evaporation took only a few seconds using a laser cutter, and the pattern can very easily be modified when necessary.

Preparing the substrates took the same amount of time, as with the conventional method, the elastomer was cured in the 3-D printed mold, while with thermal evaporation, the substrate was preliminarily prepared before patterning.

The addition of the conductive material was processed in different ways. The former case used injection of liquid metal. This step takes 5~10 mins in general but has a high probability of failure because excessive pressure causes liquid leakages. The other method used thermal evaporation. Assuming a deposition rate of 1 Å/s, a minimum thickness of 2100 Å was required (200Å of Ti / 400Å of In / 1500Å of Ga), and this takes 2100 s, which is 35 minutes.

The total time required by the conventional soft sensor fabrication method is 8~9 hours from the beginning to the end. In contrast, the time required for the thermal evaporation method is approximately five hours due to the reduced time required during the patterning step. In fact, numerous PDMS substrates can be prepared and cured at once, and the actual time required to fabricate soft sensors is less than one hour. Moreover, the novel method introduced here does not require manual processes such as an injection of liquid metal, making it feasible for automation.

TABLE 2

Comparison of Manufacturing Time

Fabrication Method / Compare Listing	Conventional Soft Sensor Fabrication		Thermal Evaporation Method	
	Contents	Time	Contents	Time
Patterning	3-D Printed Mold	3~4HR	Preparing Substrate (Curing Elastomer)	4HR
	Curing Elastomer at 65°C	4HR	Laser cutting	Within 1 Min
Addition of Conductive Material	Liquid Metal Injection	10Min	Evaporation of Ga and In	approximately 35 Min
Total Time Consumption		8~9HR		5HR

Chapter 5. Conclusion

In this paper, a deposition method for liquid metal thin-film patterns for stretchable electronics using thermal evaporation is proposed. A soft sensor was created with a PDMS substrate and patterned with a Kapton tape shadow mask designed using a laser cutter. The conductive materials of gallium and indium were thermally evaporated and laminated with the help of a titanium sacrificial layer and the substrate engraved to increase the surface roughness.

Although this fabrication method still has room for improvement in the sensing performance [36], this is a meaningful study in that it demonstrates the possibility of an automated and mass-producible process. An immediate future task is to improve the performance of

the sensor, and the fabrication of various shapes of sensor can be realized to exceed those by the conventional method of fabricating soft sensors. Thus far, the sensor fabricated here focuses on imitating the conventional sensor. In the future, various types of sensors will be required to verify the fabrication method proposed here. Other future work will be to use a different shadow mask. Kapton tape patterned with a laser cutter is limited in terms of the width of the channel. By using a laser with better precision and using a different material for the shadow mask, the resolution of the soft sensor can be improved. Finally, tests of the sensor lifetime and fatigue characteristics will be necessary in the future.

Bibliography

(1)Amjadi, Morteza, Yong Jin Yoon, and Inkyu Park. "Ultra-stretchable and skin-mountable strain sensors using carbon nanotubes-Ecoflex nanocomposites." Nanotechnology 26.37 (2015): 375501. S

(2)Lu, Nanshu, et al. "Highly sensitive skin-mountable strain gauges based entirely on elastomers." Advanced Functional Materials 22.19 (2012): 4044-4050.

(3)Xu, Feng, and Yong Zhu. "Highly conductive and stretchable silver nanowire conductors." Advanced materials 24.37 (2012): 5117-5122.

(4)Amjadi, Morteza, et al. "Highly stretchable and sensitive strain sensor based on silver nanowire-elastomer nanocomposite." ACS nano 8.5 (2014): 5154-5163.

(5)Muth, Joseph T., et al. "Embedded 3D printing of strain sensors within highly stretchable elastomers." Advanced Materials 26.36

(2014): 6307-6312.

(6)Lee, Hyungdong, et al. "Directly printed stretchable strain sensor based on ring and diamond shaped silver nanowire electrodes." Rsc Advances 5.36 (2015): 28379-28384.

(7)Hempel, Marek, et al. "A novel class of strain gauges based on layered percolative films of 2D materials." Nano letters 12.11 (2012): 5714-5718.

(8)Luo, Sida, and Tao Liu. "Structure-property-processing relationships of single-wall carbon nanotube thin film piezoresistive sensors." Carbon 59 (2013): 315-324.

(9)Lu, Nanshu, et al. "Highly sensitive skin-mountable strain gauges based entirely on elastomers." Advanced Functional Materials 22.19 (2012): 4044-4050.

(10) Mattmann, Corinne, Frank Clemens, and Gerhard Tröster. "Sensor for measuring strain in textile." Sensors 8.6 (2008): 3719-3732.

(11) Bae, Sang-Hoon, et al. "Graphene-based transparent strain sensor." Carbon 51 (2013): 236-242.

(12) Wang, Yan, et al. "Wearable and highly sensitive graphene strain sensors for human motion monitoring." Advanced Functional Materials 24.29 (2014): 4666-4670.

(13) Yamada, Takeo, et al. "A stretchable carbon nanotube strain sensor for human-motion detection." Nature nanotechnology 6.5 (2011): 296.

(14) Cohen, Daniel J., et al. "A highly elastic, capacitive strain gauge based on percolating nanotube networks." Nano letters 12.4 (2012): 1821-1825.

(15) Liu, Chao-Xuan, and Jin-Woo Choi. "Analyzing resistance response of embedded PDMS and carbon nanotubes composite under tensile strain." Microelectronic Engineering 117 (2014): 1-7.

(16) Mengüç, Yiğit, et al. "Wearable soft sensing suit for human gait measurement." The International Journal of Robotics Research 33.14 (2014): 1748-1764.

(17) Rus, Daniela, and Michael T. Tolley. "Design, fabrication and control of soft robots." Nature 521.7553 (2015): 467.

(18) Chossat, Jean-Baptiste, et al. "A soft strain sensor based on ionic and metal liquids." IEEE Sensors Journal 13.9 (2013): 3405-3414.

(19) Zhou, Y. X., et al. "Simple fabrication of molecular circuits by shadow mask evaporation." Nano letters 3.10 (2003): 1371-1374.

(20) Zhou, Yinhua, et al. "Direct correlation between work function of indium-tin-oxide electrodes and solar cell performance influenced by ultraviolet irradiation and air exposure." Physical Chemistry Chemical Physics 14.34 (2012): 12014-12021.

(21) Delcorte, Arnaud, et al. "Improvement of metal adhesion to silicone films: a ToF-SIMS study." Adhesion aspects of thin films 2 (2005): 155-221.

(22) Bhattacharya, Shantanu, et al. "Studies on surface wettability of poly (dimethyl) siloxane (PDMS) and glass under oxygen-plasma treatment and correlation with bond strength." Journal of microelectromechanical systems 14.3 (2005): 590-597.

(23) Toepke, Michael W., and David J. Beebe. "PDMS absorption of small molecules and consequences in microfluidic applications." Lab on a Chip 6.12 (2006): 1484-1486.

(24) Kato, Hirofumi, et al. "Bonding of alkali-and heat-treated tantalum implants to bone." Journal of Biomedical Materials Research: An Official Journal of The Society for Biomaterials, The Japanese Society for Biomaterials, and The Australian Society for Biomaterials and the Korean Society for Biomaterials 53.1 (2000): 28-35.

(25) Chu, Paul K., et al. "Plasma-surface modification of

biomaterials." Materials Science and Engineering: R: Reports 36.5-6 (2002): 143-206.

(26) Schweikart, Alexandra, et al. "Controlled wrinkling as a novel method for the fabrication of patterned surfaces." Complex Macromolecular Systems I. Springer, Berlin, Heidelberg, 2009. 75-99.

(27) Johnston, I. D., et al. "Mechanical characterization of bulk Sylgard 184 for microfluidics and microengineering." Journal of Micromechanics and Microengineering 24.3 (2014): 035017.

(28) Park, Yong-Lae, Bor-Rong Chen, and Robert J. Wood. "Design and fabrication of soft artificial skin using embedded microchannels and liquid conductors." IEEE Sensors Journal 12.8 (2012): 2711-2718.

(29) Tsang, W. T., and M. Ilegems. "Selective area growth of GaAs/Al x Ga1- x As multilayer structures with molecular beam epitaxy using Si shadow masks." Applied Physics Letters 31.4 (1977): 301-304.

(30) Egger, Stefan, et al. "Dynamic shadow mask technique: A

universal tool for nanoscience." Nano letters 5.1 (2005): 15-20.

(31) Yilbaş, Bekir S. "Experimental investigation into CO2 laser cutting parameters." Journal of Materials Processing Technology 58.2-3 (1996): 323-330.

(32) Dickey, Michael D., et al. "Eutectic gallium-indium (EGaIn): a liquid metal alloy for the formation of stable structures in microchannels at room temperature." Advanced Functional Materials 18.7 (2008): 1097-1104.

(33) Bae, Seung Yong, et al. "Comparative structure and optical properties of Ga-, In-, and Sn-doped ZnO nanowires synthesized via thermal evaporation." The Journal of Physical Chemistry B 109.7 (2005): 2526-2531.

(34) Laflamme, Simon, et al. "Soft capacitive sensor for structural health monitoring of large-scale systems." Structural Control and Health Monitoring 19.1 (2012): 70-81.

(35) Bogue, Robert. "3D printing: the dawn of a new era in manufacturing?." Assembly Automation 33.4 (2013): 307-311.

(36) Muth, Joseph T., et al. "Embedded 3D printing of strain sensors within highly stretchable elastomers." Advanced Materials

26.36 (2014): 6307-6312.

Abstract

소프트 로봇의 발전은 높은 유연성, 내구성, 생체 적합성 및 가벼운 무게 등의 특성을 지닌 장점으로 인해, 다양한 분야에서 활용되기 시작되었다. 그리고 그 영향으로 소프트 센서의 필요성도 점차 높아지고 있는 추세이다. 이러한 대부분의 소프트 전자장치의 제조 방법은 수동 공정이며, 많은 시간을 요구한다. 본 논문에서는 소프트 센서의 높은 수요의 요구사항을 만족하는 자동화 대량 생산 방법을 위해, 그리고 기존의 수작업 방식의 제조 방법을 개선시키기 위해서, 열 증발을 이용한 소프트 센서의 새로운 제조 방법을 제안한다. 기존의 액체를 다루었던 소프트 센서의 제조 과정에 비해, 고체를 컨트롤 하는 많은 이점을 가지고 있는 이 제조 공정은 종래의 제조 공정에 비해 공정 단계가 간단하므로 시간이 훨씬 적게 소요되며, 비용도 적게 든다. 또한, 수동 공정이 필요 없기 때문에 자동화 공정 및 대량 생산이 가능하다. 기존의 제조 방법의 소요시간은 8~9시간인데 비해, 이 연구에서 제안된 열 증착 방식을 이용한 제조 공정은 4~5시간이 소요된다. 그리고 또한 기존의 액체를 다루었던 공정과정이 작업공간을 많이 오염시키는데 비해, 고체를 다룬다는 점에서 작업환경을 깨끗하게 유지 할 수 있고, 완성품의 청결도도 우수하다. 본 논문은 기존의 소프트 센서의 제조방법과 새롭게 제시되는 열 증발 방식에 의한 제조 방법을 비교한다. 1장은 연구 시작 배경과 전체 제조 방법에 대한 요약입니다. 2장에서는 전체 제조 공정을 단계별

로 설명하고 직면 한 문제와 그 해결 방법을 설명합니다. 3장은 열 증착을 통해 최종적으로 완성된 센서와 그 특성에 대한 결과이다. 제 4장에서는 기존의 분사 방식과 제안 된 방식을 비교한다. 마지막으로, 제5장에서는 연구의 강점과 약점을 결론 짓고 미래 연구가 제안된다.